

¹ Beijing Key Lab for Terahertz Spectroscopy and Imaging;
Key Laboratory of Terahertz Optoelectronics, Ministry of Education;
Department of Physics, Capital Normal University
Beijing, China 100048

² School of Optoelectronics, Beijing Institute of Technology
Beijing, China 100081

APPLICATION OF TERAHERTZ SPECTROSCOPY AND IMAGING

We examined the feasibility of Terahertz time-domain spectroscopy (THz-TDS) using a 4-mm-thick quartz crystal to extract the angle of rotation of THz radiation polarization induced by a two-color laser in air plasma. We also used the THz-TDS technique to identify explosives and melamine in mixtures. In addition, we presented a new opto-mechanical scanner for security applications using the method of passive THz imaging.

Keywords: THz, spectroscopy, passive imaging.

Му Кайюн, Жанг Кунлин

ПРИМЕНЕНИЕ ТЕРАГЕРЦОВОЙ СПЕКТРОСКОПИИ И ВИЗУАЛИЗАЦИЯ

Мы исследовали применимость терагерцевой спектроскопии с разрешением по времени (THz-TDS) с использованием кварцевого кристалла толщиной 4 мм для получения угла вращения поляризации ТГц излучения, создаваемой двухцветным лазером в воздушной плазме. Мы также использовали эту технику THz-TDS для обнаружения взрывчатых веществ и меламин в смесях. Кроме этого, мы представили новый оптико-механический сканер с использованием метода пассивной ТГц визуализации для целей обеспечения безопасности.

Ключевые слова: ТГц, спектроскопия, пассивная визуализация.

1. Introduction

In the past two decades THz waves have attracted much attention. Their unique characteristics, e.g. non-invasiveness, low-energy, high-penetrability and spectral selectivity, favor a number of applications to the fundamental science, industry, bio-medication, national security, etc^[1-4]. In this paper, we focused on the applications of the THz-TDS technique, passive THz imaging and THz polarization detection in the field of contraband material detection and security inspection.

2. THz spectroscopy

2.1 THz wave polarization analyzer

THz wave polarization is critical in studying the THz wave properties, generation mechanism, and information processing. Here we present a convenient THz wave polarization

analyzer using a birefringent quartz crystal for extracting the polarization angle of linearly polarized wave from a single measurement of ordinary (*o*) and extraordinary (*e*) rays.

It should be pointed out that the analyzer used in experiment must have a relatively low absorption in the THz region, and it should be thick enough to separate the *o* and *e* rays beyond a one-cycle THz pulse. Since in the THz frequency range the absorption coefficients of quartz for the *o* and *e* rays are similar and lower than 0.5 cm^{-1} , their refractive indices increase with the frequency and are below $2.1^{[5]}$. The medium birefringence and relatively small absorption loss allowed neglecting the attenuation caused by the different absorption and reflection losses for both axes. So, in our experiment we used a 4-mm-thick quartz as a polarization analyzer.

When a THz pulse is measured using electro-optic sampling, it is assumed that the (001)

axis of (110)-oriented ZnTe is fixed in the vertical direction. If the polarization of probe beam is horizontal, then only the horizontally polarized THz electric field component is detected. The measured arbitrary THz polarization angle α with respect to the horizontal direction is

$$\alpha = \arccos\left(\frac{\Delta I(\alpha)}{\Delta I_{\max}}\right), \quad (1)$$

where $\Delta I(\alpha)$ is the measured current intensity difference and ΔI_{\max} is the maximum intensity difference at rotation of the THz polarization through at least a half-circle.

When a linearly polarized THz pulse \hat{e}_i at an angle θ to the horizontal direction (x axis) passes through a birefringent crystal directed at 45° , the absorption and reflection loss neglected, it is decomposed into two vector components with polarizations parallel and perpendicular to the optical axis of the analyzer (Fig.1(a)). Each part travels through the birefringent crystal, producing o or e rays of similar shape to the reference beam. Since the detector is only sensitive to the horizontal polarization, the detected signal is proportional to the projec-

tion of the outgoing field on the horizontal axis.

The THz wave in this experiment is generated in plasma by a two-color laser. The generated THz wave is linearly polarized, and the polarization is varied to change the BBO-to-plasma distance [6]. As a horizontally-polarized THz pulse passes through the quartz crystal, the pulse peak splits into two peaks of comparable magnitudes. If the difference of the optical path lengths for the o and e rays is larger than the THz pulse width, the detected signal is superposed by \hat{e}_{out-o} and \hat{e}_{out-e} , appearing to be a pulse train with two distinct peaks (Fig.1(b)). If the polarization of the incident beam rotates, the orientation angle θ can be extracted from the ratio of the amplitudes of the first maximum \hat{e}_{out-o} and the second maximum \hat{e}_{out-e} of the transmitted THz signal [7]:

$$\theta = 45^\circ - \arctan\left(\frac{\hat{e}_{out-o}}{\hat{e}_{out-e}}\right). \quad (2)$$

Fig. 2 shows the THz wave polarization angles to the x axis, calculated using Eq. (2). For comparison, the angle was also calculated using Eq. (1). The good agreement of the two curves

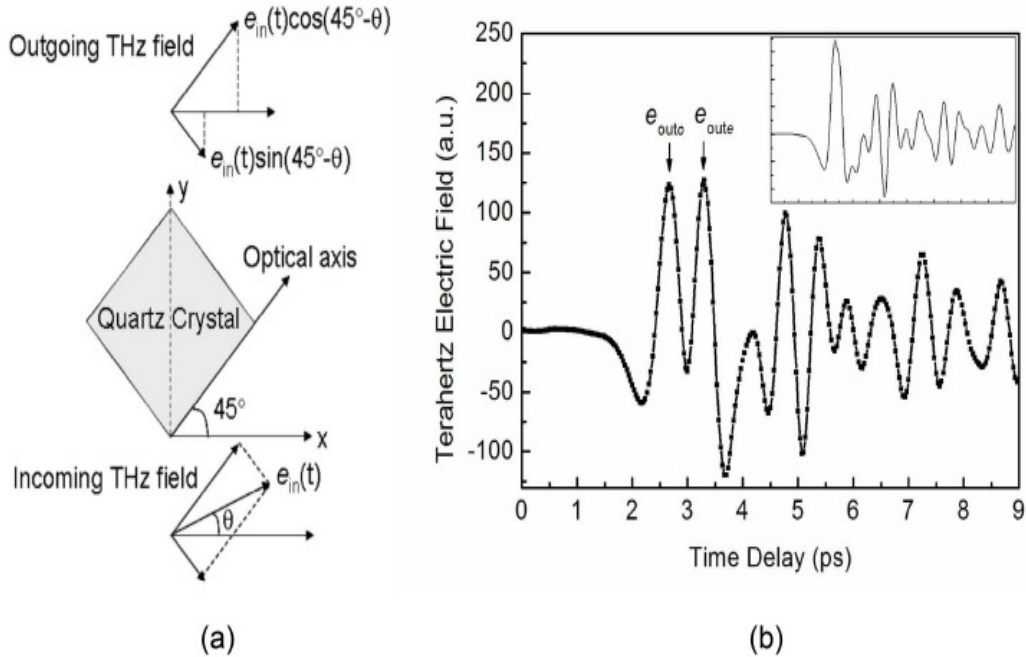


Fig. 1. (a) Orientation of the incoming THz field, the quartz crystal and the outgoing THz field. (b) THz-TDS waveform transmitted through the quartz crystal with the optical axis at 45° . The inset shows the reference THz waveform of free space

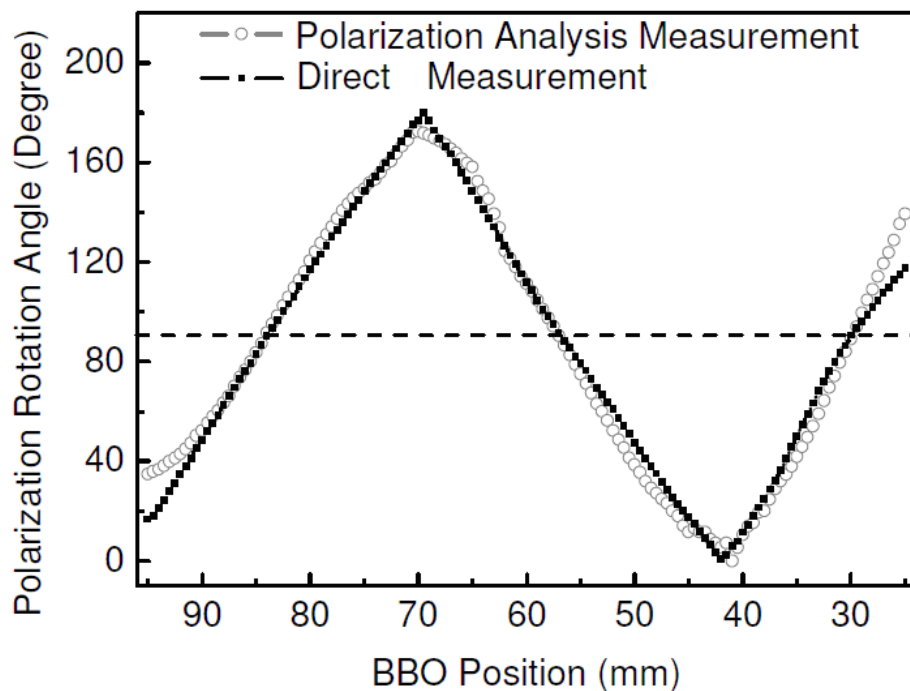


Fig.2. Angle of THz polarization rotation with respect to the x axis versus the relative phase of the two-color field, calculated using Eq. (2) (hollow circle dots) and Eq. (1) (square solid dots). The dash line indicates a 90° rotation angle

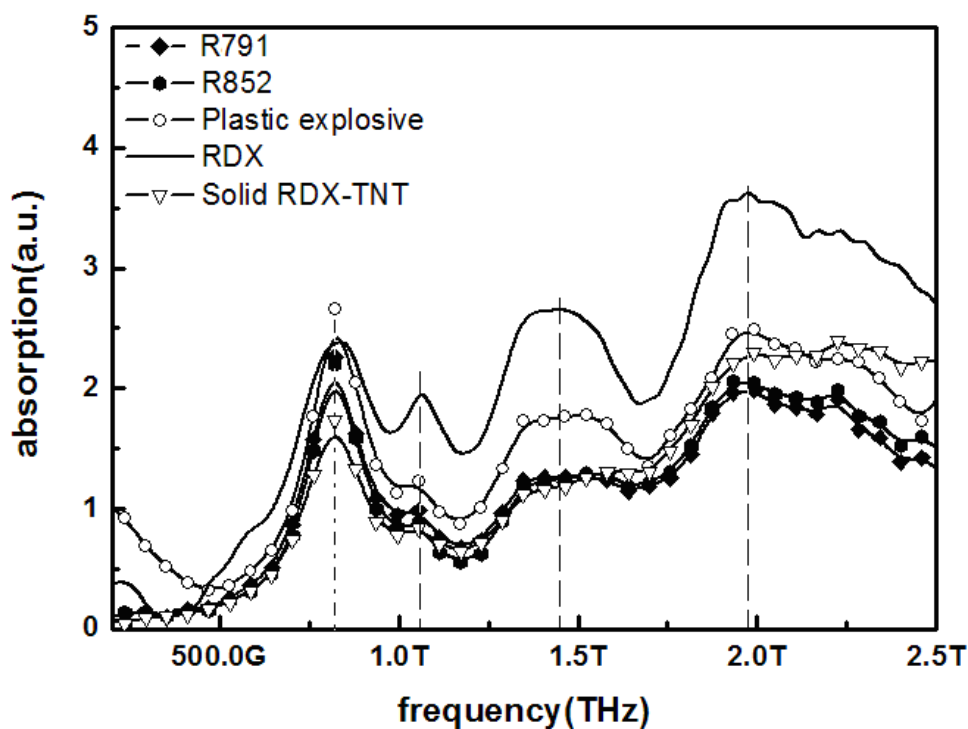


Fig.3. Absorption spectra of RDX and the four mixtures

indicates the validity of this method. In addition, this method is more convenient and time-efficient because it requires a single measurement. Meanwhile, it is more reliable due to the measurement of the difference in the amplitude of two peaks, each maintaining a sufficient signal-to-noise ratio during one rotation cycle, which enables high sensitivity of the method in detecting subtle polarization variations.

2.2 Inspection of contraband material

When THz photons are emitted or absorbed, the thermal, rotational, vibrational or bending state of molecules within a material will change. THz spectroscopy is able to provide information on the molecular properties regarding the chemical and physical processes during reactions.

The THz-TDS technique can measure the change in the time-resolved electric fields of THz pulses propagating through a sample and the equivalent length of free space. In addition, most materials have their spectral fingerprints in the THz band. So we can recognize them in mixtures.

RDX, also known as hexogen, is an explosive that is widely used in military and industrial applications. RDX is usually used in mixtures with other explosives or chemical components, which can improve its explosive power. We have used the THz-TDS technique to measure the RDX and four other composite explosives (R791, R852, plastic explosive, and solid RDX-TNT), the main component of

which is RDX (Fig.3). Fig.3 shows the agreement of the THz spectra of RDX and the other four explosives. It does indicate that THz-TDS technique is able to pick up RDX from other materials.

Melamine is an industrial raw material which is widely applied to the production of durable thermosetting plastics, flame-retardant materials, and other products. Melamine was found in some food products, e.g. milk powder, in China recently. Although a melamine additive can improve the protein content in food, it is harmful to human health. Ingestion of melamine may damage the human urinary system, resulting in kidney stones and induced bladder cancer. Infants and young children are more vulnerable to melamine. Excessive intake of melamine can even cause death^[8].

In order to verify the applicability of the THz-TDS technique to the detection of melamine, some mixtures of melamine and milk powder were measured. Pure milk powder and its mixtures with 1%, 2%, 5%, 10%, 20% and 30% of melamine were used as samples. The absorption coefficients were calculated from the time-domain spectrum. Their plots are presented in Fig.4. The absorption line was shifted for clarification. Because of the strong absorption in milk powder, the terahertz waves were excessively absorbed by mixtures with less than 5% melamine content, and the absorption in milk powder flooded that in melamine. When the proportion of melamine increased above 10%, the absorption peaks at 1.99 and 2.29THz could be observed.

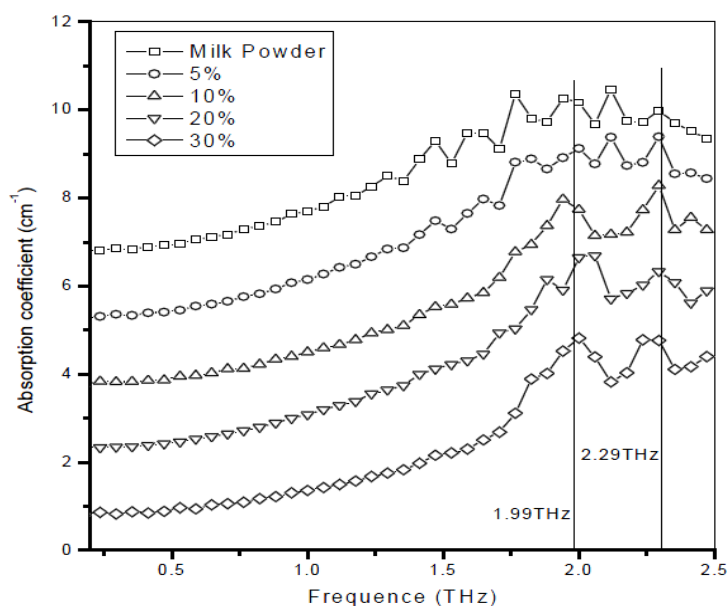


Fig.4. Absorption coefficient of mixtures of melamine and milk powder in different proportions

3. THz imaging

We describe a new opto-mechanical THz scanner which is promising as for the application of THz imaging to the national security. In the future this scanner may be used for portal screening of concealed weapons. This setup can be used both for active and passive THz imaging.

Up to the present the most widely adopted THz imaging system has worked in a raster scan fashion, which is unpractical for real applications. 2D THz array detectors can be applied to real time imaging. However, at present their cost is prohibitively high. Fortunately, a low-cost, high-performance, opto-mechanical scanner is able to meet the current requirements. An opto-mechanical scanner is able to rapidly scan a 2D image of a sample. It also has high optical efficiency and thus an image system can achieve the required thermal sensitivity with a minimum number of receivers. Therefore, it can easily operate at any wavelength and be active or passive. The opto-mechanical scanning can meet these requirements and is constantly improved for creation of a best-performance, low-cost prototype system that will meet the future needs for THz security applications.

The opto-mechanical THz scanner includes three parts: the line scan group, which consists of a pair of plane mirrors that are rotating simultaneously but in opposite directions, a flapping mirror, which not only is flapping in the vertical direction but also rotating in azimuth,

and a concave mirror that can collect the THz waves from the sample and focus them on the imaging front-end.

When the two plane mirrors of the line scan group rotate with the same speed but in opposite directions and the axes of rotation are normal, the spot of imaging is fixed in one position. When the axis of rotation is tilted with respect to the normal, the spot of imaging, which is reflected by the two rotating plane mirrors, will have an offset in the line scan section. The tilt angle is determined by the scanning range and the distance between the rotating mirror and the imaged sample. As there are mutual compensations between the two rotating mirrors, the position of imaging in the meridional plane will not change. In the sagittal plane, however, the position of imaging will change as the tilt directions of the two rotating mirrors are opposite and thus there is an additional offset. The direction and size of the offset of the position of imaging will change with the rotation of the mirrors. So, the orbits of imaging will be a line when the spot of object is fixed. According to the principle of optical reversibility, when the spot of imaging is fixed, the spot of object will change and the orbits will be a line. The length of the line is determined by the tilt angle of rotation and the distance between the rotating mirror and the imaged sample.

As regards the performance of the scanner, the spatial resolution was same as the theoretically calculated, i.e. 3.8° , and the spot size was 10cm at a distance to the subject of 1.5m.

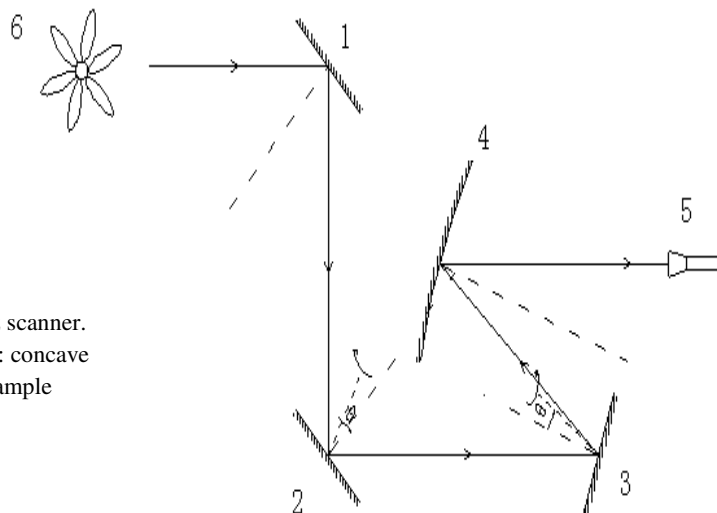


Fig.5. Sketch of the opto-mechanical THz scanner.
1: flapping mirror; 2, 3: rotating mirror; 4: concave mirror; 5: imaging front-end; 6: imaged sample



Fig. 6. Photo of the opto-mechanical THz scanner

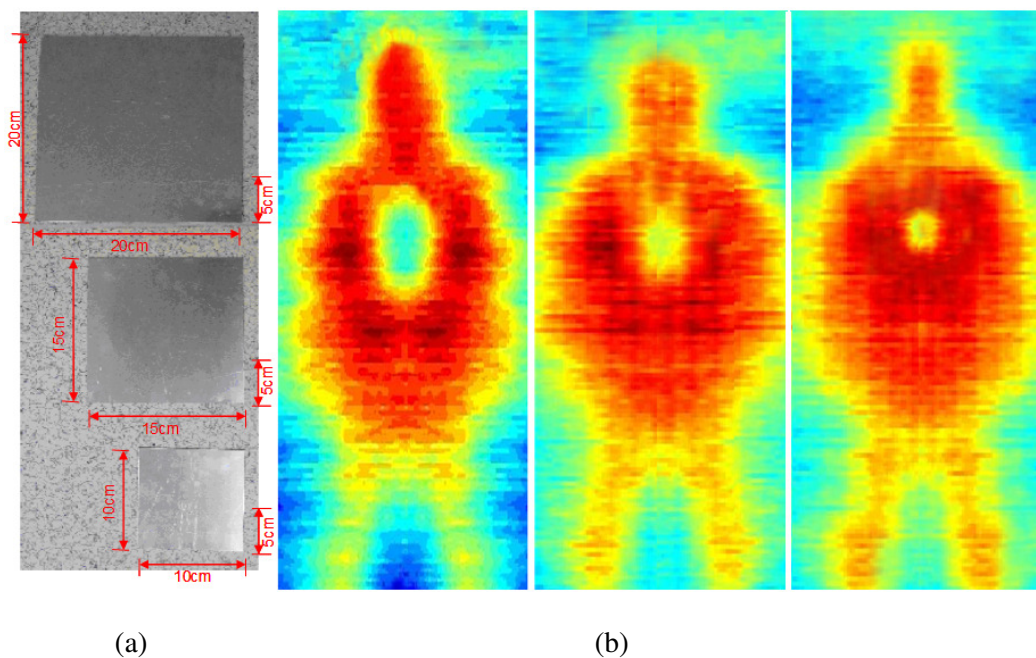


Fig.7. (a) Photo of three aluminum plates of different size. (b) Passive imaging result

The photo of the opto-mechanical THz scanner is shown in Fig. 6, and the passive imaging results are shown in Fig. 7. Fig. 7 (a) is the photo of three aluminum plates of different

size, which are concealed in the clothes. Fig. 7 (b) is the passive THz imaging result. From the above images one can identify the profile of the person and the aluminum plates. However, de-

tails of the person, e.g. arms, legs and facial features, can not be resolved because the spatial resolution of this scanner is only 10cm.

Conclusion

In numerous cases, laboratory tests of the feasibility of specific THz spectroscopy and imaging applications have shown great prospects, and in a few cases these tests have led to more realistic field tests. For the technology to gain more widespread acceptance, a great deal of research is needed. The terahertz radiation seems to be a vibrant and active field for many years to come.

References

[1] *Eric Freysz and Jérôme Degert*, Terahertz Kerr effect, *Nature Photonics*, 4, 131-132, 2010.
[2] *Irl Duling and David Zimdars*, Terahertz imaging revealing hidden defects, *Nature Photonics*, 3, 630- 632, 2009.

[3] *B.S. Alexandrov, V. Gelev, et al*, DNA breathing dynamics in the presence of a terahertz field, *Physics Letters A*, 374, 1214-1217, 2010.

[4] *John F. Federici, Dale Gary, et al*, THz standoff detection and imaging of explosive and weapons, *Proc. of SPIE* 5781, 75, 2005.

[5] *L. Zhang, H. Zhong, et al*, Polarization sensitive terahertz time-domain spectroscopy for birefringent materials, *Appl. Phys. Lett*, 94, 211106, 2009.

[6] *H. Wen and A. M. Lindenberg*, Coherent terahertz polarization control through manipulation of electron trajectories, *Phys. Rev. Lett.* 103, 023902, 2009.

[7] *Liangliang Zhang, Hua Zhong, et al*, Terahertz wave polarization analyzer using birefringent materials, *Optics Express*, 17(22), 20266, 2009.

[8] *Ye Cui, Kaijun Mu, et al*, Measurement of mixtures of melamine using THz ray, *Proc. of SPIE*, 7385, 2009.

10.09.2010